Red persistent luminescence excited by visible light in CaS:Eu^{2+},Tm^{3+}

Yuki Tamura[1], Tsuyoshi Okuno[1], Yoriko Suda[2], Yasushi Nanai[3]

[1] Department of Engineering Science, The University of Electro-Communications, Chofu, Tokyo 182-8585, Japan

[2] School of Engineering, Tokyo University of Technology, Tokyo 192-0982, Japan

[3] Department of Electrical Engineering and Electronics, Aoyama Gakuin University, 5-10-1 Fuchinobe, Chuo-ku, Sagamihara-shi, Kanagawa 252-5258, Japan

E-mail: t1933086@edu.cc.uec.ac.jp okunotsuyoshi@uec.ac.jp

Abstract

Excitation wavelength dependence of red persistent luminescence in CaS:Eu^{2+},Tm^{3+} phosphor is reported. Persistent luminescence appears under visible light excitation in the wavelength region of 400-600 nm. Photon energy from white light-emitting diode lamps is possibly stored in this material. This sulfide phosphor is synthesized using iodine vapor. Under iodine vapor, Eu^{2+} and Tm^{3+} are found to be efficiently included in CaS. The concentration dependence of Eu^{2+} is studied, and the optimum concentration is 0.05%. Trap depth of 0.27-0.33 eV contributing to persistent luminescence is evaluated by using thermoluminescence.

Key Words

luminescence, afterglow, phosphor, sulfide, europium, thermoluminescence

1. Introduction

Research on phosphor materials has been one of important themes for low energy consumption [1]. High-efficiency optical materials contribute to energy saving lighting. In addition, persistent luminescence phenomenon has attracted attention for application in safety indication, soft illumination, medical imaging, and so on. Some phosphors such as $SrAl_2O_4:Eu^{2+},Dy^{3+}$ give luminescence for several minutes or hours even after ceasing of photoexcitation [2]. Persistent luminescence phosphors are used for safety signage, and expected for safety guidance especially at a blackout. Even more efficient persistent luminescence phosphors, if they are realized, could be useful for display or lighting at night. This comes to be storage of daytime or lighting energy, and reuse of it without battery or electricity. Intense persistent luminescence and a proper on-off cycle of display backlight could bring about quite low energy consumption in display. Exploring and improving persistent luminescence continually attract attention of relevant researchers [3-12].

One of the most famous persistent phosphors is $SrAl_2O_4:Eu^{2+},Dy^{3+}$ [2]. This green luminescence material is efficiently excited by photons in near ultraviolet (UV) region. Energy storage is effectively achieved using photons having wavelength less than 400 nm. Light emitting diodes (LEDs) are currently used for lighting devices. Spectra of ordinary white LED lamps consisting of blue LEDs and yellow phosphors do not have UV wavelength region. Efficient photoexcitation or energy storage of present persistent phosphors becomes difficult in modern LED light. In addition, color of present persistent phosphors is almost limited to green or blue. Examples of blue persistent phosphors are $Sr_2MgSi_2O_7:Eu^{2+},Dy^{3+}$ [13] and $CaAl_2O_4:Eu^{2+},Nd^{3+}$ [14], which have persistent luminescence duration similar to $SrAl_2O_4:Eu^{2+},Dy^{3+}$. However, red or orange phosphors having intense and long persistent luminescence are lacking. An example is $Y_2O_2S:Eu^{3+},Ti^{4+},Mg^{2+}$ in which the intra $4f^6$ transition of Eu^{3+} at 627 nm gives persistent luminescence [15]. Another example is the intra $4f^5$ transition of Sm^{3+} at 618 nm in $SnO_2:Sm^{3+},Zr^{4+}$ [16] or $ZrO_2:Sm^{3+},Sn^{4+}$ [17]. Further improvement of intensity and duration of persistent luminescence of red phosphors is demanded. Vast usage of red persistent phosphors is not realized. Therefore, white persistent

luminescence, that is, lighting by persistent luminescence is not at all obtained. White persistent phosphors with one kind of luminescence center in single compound are also tried to be developed. Persistent luminescence bands in $Sr_3Al_2O_5Cl_2:Eu^{2+},Dy^{3+}$ are located at 450 nm and 550 nm [18]. In addition, reports of UV persistent phosphors, which is quite important for excitation of visible white light as well as disinfecting field, are limited [7,19]. Further study on white persistent phosphors is also necessary for longer luminescence duration and practical applications.

$CaS:Eu^{2+},Tm^{3+}$ is a well-known phosphor which emits in the red [20]. The origin of the intense red luminescence is the $5d^14f^6$-$4f^7$ transition of Eu^{2+} in CaS or SrS, and its persistent luminescence have been studied [20-25]. An advantage of persistent luminescence of $CaS:Eu^{2+}$ is a broad absorption band in visible wavelength region. Excitation spectrum for the red photoluminescence (PL) ranges from 400 to 600 nm, which corresponds to the transition from the ground $4f^7$ state to the upper $5d^14f^6$ state. $CaS:Eu^{2+}$ is possibly be good persistent phosphor in which the energy is stored by visible light. Excitation spectrum for persistent luminescence in $CaS:Eu^{2+}$ is not reported so far. In this paper, optical properties of $CaS:Eu^{2+},Tm^{3+}$ are studied. It is found, for the first time to the authors' knowledge, that iodine (I_2) vapor is useful for including Eu^{2+} into CaS. Concentration dependence of Eu^{2+} is studied, and the optimum atomic ratio of Eu to Ca is found to be 0.05%. The intensity of thermoluminescence (TL) is larger for this Eu concentration, and duration of persistent luminescence excited at 442 nm is 700 s. Excitation spectrum for persistent luminescence is confirmed to be the same as excitation spectrum for PL.

2. Experimental

For the fabrication of $CaS:Eu^{2+},Tm^{3+}$ powders, we used solid-state reaction technique in a quartz tube [26-29]. A mixture of CaS, EuS and Tm_2S_3 in the atomic ratio of $Ca^{2+} : Eu^{2+} : Tm^{3+} = 1 : x : 0.02$ was prepared. The total weight of the powder was approximately 600 mg. The value x refers to the concentration of Eu^{2+} in the range of 1×10^{-4}-1×10^{-2}, and the samples are denoted as Eu0.01%-Eu1% in this paper. To promote the addition of europium ions, 300 mg of iodine was

added to the mixture of the starting materials. Iodine vapor is useful for including Eu^{2+} into CaS. The mixture powder was placed in the center of the quartz tube whose diameter and length are 20 mm and 1 m, respectively. The ends of the tube were closed and the tube was evacuated to a pressure of ~50 Pa. The center of the tube was heated by a cylindrical furnace at 1100°C for 24 h. The length of the furnace is 0.3 m, and thus the most of iodine became a solid quickly at the room-temperature region in the both ends of the quartz tube.

X-ray diffraction (XRD) patterns were recorded using a Rigaku Rint2200-UltimaIII diffractometer. PL spectra were measured using an Oriel MS257 spectrometer equipped with an Andor Technology DH734-18F charge-coupled-device camera. Internal quantum efficiency was measured with a Hamamatsu C11347-01 spectrophotometer equipped with an integrating sphere. Sample powder (~10 mg) was put on a quartz Petri dish which was placed within the integrating sphere. Monochromatic output of a xenon arc lamp was used for the excitation. Sample absorption was evaluated from the decrease in the excitation intensity by the presence of the sample, comparing the excitation intensity without the sample. The internal quantum efficiency corresponds to the photon-number ratio of luminescence to absorption. Afterglow decay curves of persistent luminescence were measured using the apparatus used for the PL measurement. The afterglow time is defined as the time for the luminance to reach 0.32 mcd/m^2. This value is the lowest luminance human eyes can see. Afterglow decay curves were measured after irradiation of visible light for 10 min. The luminance value was evaluated by a Topcon BM-7AS luminance meter. For TL measurements, samples were heated using a closed-cycle helium cryostat from 70 K to 600 K. At 70 K, sample powder was irradiated for 30 min by a UV mercury lamp (254 nm, Panasonic GL-6, 6 W) or a blue LED (470 nm, OptoSupply OSB5XNE3C1S, 3 W). Then the

sample was heated with the ratio of 3, 5, or 10 K/min. The TL signal was recorded with a Hamamatsu R374 photomultiplier tube.

3. Results and discussions

Figure 1 shows the XRD patterns of the CaS:Eu^{2+},Tm^{3+} phosphors. The Eu atomic ratio is shown in the figure. In the lower part of the figure, the patterns of powder diffraction files (PDF) of CaS, Tm_2O_3, and CaO are included. The cubic structure with a space group of $Fm\bar{3}m$ (no 225) for CaS is shown. Even when the Eu ratio increases from 0.01% to 1%, angles of XRD peaks do not change. The lattice constants do not change. This result implies that the crystal structure of CaS is not affected by the addition of Eu^{2+} ions. Small traces of the XRD peaks of CaO and Tm_2O_3 are recognized. Residual oxygen in the quartz tube in the heating process slightly affected the sulfide synthesis. Complete suppression of CaO and Tm_2O_3 XRD peaks is not succeeded at present. Small XRD peaks of Tm_2O_3 are always present and some constant amount of the starting ratio of Tm^{3+} (2% of Ca^{2+}) is considered to be included in the CaS:Eu^{2+},Tm^{3+} phosphors. The intensity of CaO XRD peaks slightly changed depending on the synthesis duration at 1100ºC. No clear correlation between the residual CaO and afterglow phenomena discussed below is found. In this paper, experiments are conducted using the 24-h synthesis duration for all of the samples, assuming that the effect of CaO is negligible or constant among the samples.

Figure 2 shows the PL and its excitation (PLE) spectra of the CaS:Eu^{2+},Tm^{3+} phosphors. The excitation for PL was obtained by using monochromatic output of a xenon arc lamp (500 W, Ushio Ui-501C) at 460 nm. Upon visible light irradiation, red emission at 650 nm originating from the $5d^14f^6$ - $4f^7$ transition of the Eu^{2+} ion was observed on all the samples. In these phosphors, Eu^{2+} ions act as luminescent centers. In all of the PL spectra, the small dip is observed at 690 nm. This

is considered to be absorption of Tm^{3+} doped in CaS. This wavelength corresponds to the transition from the ground $^3H_6$ to the upper $^3F_3$ state of Tm^{3+} according to the Dieke diagram [30]. The concentration of Tm^{3+} is 2%, and PL of Eu^{2+} is slightly absorbed at 690 nm by Tm^{3+}. Similar dips coming from absorption of rare earth ions in PL spectra are also reported for Pr^{3+} doped ZnO [26]. The PLE spectra in figure 2 indicate that the CaS:Eu^{2+},Tm^{3+} phosphor has an excitation band in the visible light region. This phosphor emits luminescence upon excitation with 400-600 nm light.

In figure 3, the internal quantum efficiency is plotted against the concentration of Eu^{2+} for CaS:Eu^{2+},Tm^{3+}. For Eu0.1%, the efficiency reached a maximum of 59% under the excitation at 455 nm. As the concentration of Eu^{2+} increases from 0.01% to 0.1%, the efficiency increases. However, when the concentration of Eu^{2+} is larger than 0.1%, the efficiency decreases. This is supposed to be due to concentration quenching. The energy photoexcited in Eu^{2+} moves among Eu^{2+} ions, and is relaxed nonradiatively without photoluminescence.

Figure 4 shows the afterglow decay curves of CaS:Eu^{2+},Tm^{3+}. A helium-cadmium laser was used for the excitation, and the phosphor powders were irradiated at 442 nm (80 mW) for 10 min before the measurements. Afterglow spectra were the same as the PL spectra shown in figure 2. Red afterglow was observed in all the samples after visible light irradiation. The afterglow time of CaS:Eu^{2+},Tm^{3+} is longer for Eu0.05%, and the duration is 700 s in figure 4. The optimum Eu^{2+} concentration was found to be 0.05% on afterglow properties. Tm^{3+} ion is generally considered to be the trapping center in this phosphor [20]. The substitution of Ca^{2+} by Tm^{3+} leads to the formation of charge defects in the crystal. The charge defects may cause decrease of the emission intensity. However, the charge defects in CaS:Eu^{2+},Tm^{3+} form new traps and are

responsible for the persistent luminescence. The Eu^{2+} concentration is related to probability of capturing electrons in the trap.

In order to understand the trapping processes, TL was measured. Figure 5 shows the TL glow curves of CaS:Eu^{2+},Tm^{3+}. Thermal peaks were observed at 270 K and 420 K. This TL profile is similar to that reported in the reference [20]. These peaks are related to the traps formed by the substitution of Ca^{2+} by Tm^{3+}. For Eu0.05%, the trap captures electrons most efficiently. The duration of the persistent luminescence for Eu0.05% was the longest in all of the samples in figure 4. This is consistent with the results shown in figure 5. Focusing on the TL peak at 420 K, the intensity of TL does not reach its maximum for Eu0.05%. The intensity is the maximum for Eu0.01% whose duration of the persistent luminescence is 600 s. The trap shown by the peak at 420 K in figure 5 is not supposed to significantly affect the duration of the persistent luminescence. The intensity of TL at 270 K is dominant for CaS:Eu^{2+},Tm^{3+}, and the trap related to this TL peak is considered to be the origin of the persistent luminescence.

Figure 6 shows excitation spectrum of persistent luminescence for Eu0.05%. The afterglow intensity at 150 s after the ceasing of photoexcitation was measured for each excitation wavelength. The excitation was carried out by using the monochromatic output of the xenon arc lamp. The intensity increases from 400 nm to 440 nm, and scarcely changes between 440 nm and 600 nm in figure 6. This profile is quite similar to the wavelength dependence of the PLE spectra shown in figure 2. All absorption wavelengths for PL contribute to the persistent luminescence. Absorption in the wavelength region from 400 nm to 600 nm is attributed to the transition from the ground $4f^7$ to the upper $5d^14f^6$ state of Eu^{2+}. The electron in the upper $5d^14f^6$ state will be transferred to the neighboring trap state. Based on this result, CaS:Eu^{2+},Tm^{3+} absorbs visible light and emits

afterglow luminescence. This persistent luminescence material CaS:Eu^{2+},Tm^{3+} can be excited by visible light or a white LED lamp.

Figure 7 shows effect of heating ratio on the TL curve of CaS:Eu^{2+},Tm^{3+}. Photoexcitation was carried out by using (a) a UV mercury lamp (254 nm) or (b) a blue LED (470 nm). The sample is Eu0.05%. In figure 7(a), the TL peak temperature moves to higher temperature gradually from 270 K to 310 K by increasing the heating rate from 3 K/min to 10 K/min. The trap depth E_T contributing to TL and persistent luminescence is expressed by

$$\frac{\beta E_T}{kT_m^2} = s \exp\left(-\frac{E_T}{kT_m}\right),$$

where β is the heating rate, k the Boltzmann constant, T_m the TL peak, and s the frequency factor or "escape frequency" [31-33]. To eliminate the unknown value s, the Hoogenstraaten method is often used. For several values of β, T_m would be experimentally obtained. When $\ln\left(\frac{T_m^2}{\beta}\right)$ is plotted against $1/T_m$, E_T is determined from a slope of a straight line fitting data points [34,35]. Its relation is shown in figure 8, and E_T is determined to be 0.27 eV. Figure 7(b) shows effect of heating ratio on the TL curve of CaS:Eu^{2+},Tm^{3+} excited by the blue LED. Similar TL glow curves are obtained in figures 7(a) and 7(b) irrelevant of excitation wavelength. A thermal peak about 300 K is obtained by excitation also with visible light. The Hoogenstraaten plot for the blue-LED excitation is also included in figure 8, and the trap depth is determined to be 0.33 eV. Different excitation wavelengths between UV and blue light bring about almost the same trap depth 0.30 ± 0.03 eV. The same traps are considered to be contribute to persistent luminescence in CaS:Eu^{2+},Tm^{3+} under UV and blue excitation. The small difference of the calculated trap depths 0.27-0.33 eV shows good reproducibility of these TL measurements. The obtained trap depth in this paper is shown to

be 0.3 eV and its uncertainty is estimated to be 0.03 eV. This depth 0.3 eV is similar to 0.2-0.3 eV obtained for CaS:Eu^{2+},Pr^{3+} [23,24]. In these references, TL measurements started from room temperature, and TL peak was located at around 400 K. Although the TL peak temperature and the additionally doped ions Pr^{3+} are different from CaS:Eu^{2+},Tm^{3+} in this paper, the same trap is considered to be formed and brings about red persistent luminescence in CaS:Eu^{2+}.

In the reference [20], the charge defects created by substituting Tm^{3+} for Ca^{2+} are considered to serve as hole traps for persistent luminescence. Tm^{3+} ions play the role of deep electron trapping centers, capturing electrons either through the conduction band of CaS or directly from the excited Eu^{2+} ions. These two processes were studied by using a 266 nm pulse laser or a green laser [20]. Two different sites of Tm^{3+} were suggested. Deep electron trapping centers can capture electrons through the conduction band under the 266 nm excitation. Another type of trapping centers can directly capture electrons from the metastable excited state of the excited Eu^{2+}. The latter type of centers was ascribed to be located near Eu^{2+} ions [20]. In the experiments in this paper, persistent luminescence takes place under visible light excitation, and thus the trapping centers locating near Eu^{2+} ions contribute to persistent luminescence.

Preliminary experiments obtaining temporal PL spectra and decay curves were performed using a 266 nm pulse laser (~10 ns pulse width) for the excitation. At 15 K, a blue PL band appeared at about 450 nm for CaS:Eu^{2+},Tm^{3+}. Its main decay time was ~10 ns, and figure 9 shows temporal PL spectra for Eu0.05% and Eu1%. Sampling window for PL in figure 9 was open at 20 ns after the 266 nm pulse excitation, and sampling duration was 50 μs. For Eu0.05% having a long afterglow (700 s), a large blue PL band is present in the wavelength region from 400 to 500 nm, in addition to the red PL band at 650 nm. In contrast, almost no blue PL band is observed in figure

9 for Eu1mol% where a short (20 s as is shown in figure 4) afterglow is present. The wavelength of the blue PL band agrees with the absorption of Eu^{2+} as is shown in PLE spectra in figure 2. Defect states may be responsible for this blue PL band and also may be responsible for afterglow phenomena. This situation, that is, defect states giving blue PL band are concerned with long (millisecond or longer) decay time in Eu^{2+}, is possibly similar in $CaS:Eu^{2+},Tm^{3+}$ to that in $CaAlSiN_3:Eu^{2+}$ [36] or $SiAlON:Eu^{2+}$ [37]. Detailed results will be reported elsewhere after further accumulation of experimental data. Defect states responsible for afterglow are also expected to be characterized by electron paramagnetic resonance as in the reference [38]. In addition to defect states, coexistence of Eu^{3+} [39] may affect the afterglow phenomena. Energy storage between Eu^{2+} and Eu^{3+} is possible for application in an xray dosimeter [40]. When PL spectra were measured at 15 K under the excitation at 266 nm pulses, several sharp PL lines are observed as is shown for Eu0.05% in figure 9. Such sharp PL lines at 462, 467 and 478 nm in figure 9 may correspond to the intra $4f^6$ transitions ($^5D_3$ - $^7F_4$, $^5D_2$ - $^7F_0$ and $^5D_2$ - $^7F_2$) of Eu^{3+} [41]. Such sharp PL lines appear only for the intense pulse excitation and are clearly observed for Eu0.05%. Anyhow, further study is necessary for determining the entity for energy storage or afterglow phenomena, as well as complicated energy transfer mechanism relevant to afterglow.

In the synthesis procedure of $CaS:Eu^{2+},Tm^{3+}$, iodine was included. Iodine vapor contributes to inclusion of rare-earth ions into CaS. When energy dispersive x-ray spectrometry was carried out on these samples using a Jeol JXA-8530F elemental composition analyzer, no signal of iodine was detected. When iodine was not used in the synthesis, the PL intensity was approximately 5 times smaller than that for the sample synthesized using iodine. Afterglow decay curves for samples synthesized not using iodine were almost the same as that using iodine. Difference was intensity of persistent luminescence and thus its duration. Therefore, iodine atom is considered not

to be left in CaS:Eu^{2+},Tm^{3+}. It was reported that CaS solid is grown by chemical vapor transport method [42]. A quartz ampoule including CaI_2 solid and S was heated in a furnace in the temperature region of 800-1100 ºC. After heating, solid CaS was grown in the region at ~800 ºC. Within the ampoule at ~1100 ºC, CaI_2 and S came to be gases, and were transported to lower temperature region. Then CaS solid were grown among I_2 gas [42]. In a similar manner, CaS:Eu^{2+},Tm^{3+} powder is considered to be synthesized under iodine vapor.

4. Conclusions

In order to obtain a longer afterglow time, we investigated the influence of the Eu/Ca atomic ratio on the luminescence properties. All the samples were prepared through the solid state reaction under iodine vapor. Red luminescence was emitted under the excitation with visible light. Eu^{2+} ions are emission centers in CaS:Eu^{2+},Tm^{3+}. Excitation spectrum for the red PL ranges from 400 to 600 nm, which corresponds to the transition from the $4f^7$ state to the upper $5d^1 4f^6$ state. The optimum Eu^{2+} concentration to maximize afterglow time is 0.05%. Afterglow time excited at 442 nm is 700 s. The intensity of TL is larger for Eu0.05%. The traps formed by substitution of Tm^{3+} ion capture electrons photoexcited in Eu^{2+} in these phosphors. Excitation spectrum for persistent luminescence is confirmed to be the same as excitation spectrum for PL. It is believed that CaS:Eu^{2+} or CaS:Eu^{2+},Tm^{3+} is a promising red persistent phosphor which can efficiently utilize the energy of LED lamps. Research on further improving properties of persistent luminescence of CaS:Eu^{2+} and similar materials is in progress.

Acknowledgments

Measurements of XRD, internal quantum efficiency and energy-dispersive x-ray spectrometry were carried out at the Coordinated Center for UEC Research Facilities in the University of Electro-Communications.

References

[1] Yen W M, Shionoya S, Yamamoto H (ed) 2007 *Phosphor Handbook* 2nd edn (Boca Raton, FL: CRC Press)

[2] Matsuzwa T, Aoki Y, Takeuchi N and Murayama Y 1996 A new long phosphorescence phosphor with high brightness, $SrAl_2O_4:Eu^{2+},Dy^{3+}$ *J. Electrochem. Soc.* **143** 2670-2673

[3] Kabe R and Adachi C 2017 Organic long persistent luminescence *Nature* **550** 384-387

[4] Van den Eeckhout K, Poelman D and Smet P F 2013 Persistent luminescence in non-Eu^{2+}-doped compounds: a review *Materials* **6** 2789-2818

[5] Van den Eeckhout K, Poelman D and Smet P F 2010 Persistent luminescence in Eu^{2+}-doped compounds: a review *Materials* **3** 2536-2566

[6] Liang L, Chen N, Jia Y, Ma Q, Wang J, Yuan Q and Tan W 2019 Recent progress in engineering near-infrared persistent luminescence nanoprobes for time-resolved biosensing/bioimaging *Nano Research* **12** 1279-1292

[7] Shi H and An Z 2019 Ultraviolet aftergrow *Nature Photonics* **13** 73-79

[8] Yang Y-M, Li Z-Y, Zhang J-Y, Lu Y, Guo S-Q, Zhao Q, Wang X, Yong Z-J, Li H, Ma J-P, Kuroiwa Y, Moriyoshi C, Hu L-L, Zhang L-Y, Zheng L-R and Sun H-T 2018 X-ray-activated long persistent phosphors featuring strong UVC afterglow emissions *Light: Science & Applications* **7** 88(11pp)

[9] Zhou D, Wang Z, Song Z, Wang F, Zhang S and Liu Q 2019 Enhanced Persistence Properties through Modifying the Trap Depth and Density in $Y_3Al_2Ga_3O_{12}:Ce^{3+},Yb^{3+}$ Phosphor by Co-doping B^{3+} *Inorganic Chemistry* **58** 1684-1689

[10] Zhang J-C, Wang X, Marriott G and Xu C-N 2019 Trap-controlled mechanoluminescent materials *Progress in Materials Science* **10** 678-742

[11] Delgado T, Afshani J and Hagemann H 2019 Spectroscopic Study of a Single Crystal of $SrAl_2O_4:Eu^{2+}:Dy^{3+}$ *J. Phys. Chem. C* **123** 8607-8613

[12] Nanai Y, Igarashi A and Kamioka H 2019 Excitation energy dependence for electron traps in $CaTiO_3$:Pr,Al single crystals *J. Phys.:Conf. Series* **1220** 012011(4pp)

[13] Lin Y, Tang Z, Zhang Z, Wang X and Zhang J 2001 Preparation of a new long afterglow blue-emitting $Sr_2MgSi_2O_7$-based photoluminescent phosphor *J. Mater. Sci. Lett.* **20** 1505-1506

[14] Teng X, Zhuang W, Hu Y, Zhao C, He H, Huang X 2008 Effrct of flux on the properties of $CaAl_2O_4:Eu^{2+},Nd^{3+}$ long afterglow phosphor *J. Alloys and Compounds* **458** 446-449

[15] Wang X, Zhang Z, Tang Z and Lin Y 2003 Characterization and properties of a red and orange Y_2O_2S-based long afterglow phosphor *Mater. Chem. Phys.* **80** 1-5

[16] Zhang J, Ma X, Qin Q, Shi L, Sun J, Zhou M, Liu B and Wang Y 2012 The synthesis and afterglow luminescence properties of a novel red afterglow phosphor: $SnO_2:Sm^{3+},Zr^{4+}$ *Mater. Chem. Phys.* **136** 320-324

[17] Zhao Z and Wang Y 2012 The synthesis and afterglow luminescence properties of a novel red afterglow phosphor: $ZrO_2:Sm^{3+},Sn^{4+}$ *J. Lumin.* **132** 2842-2846

[18] Zhang Q, Rong M, Tan H, Wang Z, Wang Q, Zhou Q, Chen G 2016 Luminescent properties of the white long afterglow phosphors: $Sr_3Al_2O_5Cl_2:Eu^{2+},Dy^{3+}$ *J. Mater. Electron.* **27** 13093-13098

[19] Yang Z, Liao J, Wang T, Wu H, Qiu J, Song Z and Zhou D 2014 Ultraviolet long afterglow emission in Bi^{3+} doped $CdSiO_3$ phosphors Materials Express **4** 172-176

[20] Jia D, Jia W, Evans D R, Dennis W M, Liu H, Zhu J and Yen W M 2000 Trapping processes in CaS:Eu^{2+},Tm^{3+} *J. Appl. Phys.* **88** 3402-3407

[21] Kojima Y, Aoyagi K and Yasue T 2007 Afterglow mechanism and thermoluminescence of red-emitting CaS:Eu^{2+},Pr^{3+} phosphor with incorporated Li^{+} ion upon visible light irradiation *J. Lumin.* **126** 319-322

[22] Sun J, Liu Z and Du H 2011 Effect of trivalent rare earth ions doping on the fluorescence properties of electron trapping materials SrS:Eu^{2+} *J. Rare Earths* **29** 101-104

[23] Mori K, Kojima Y and Nishimiya N 2013 Effect of initial Eu/Ca atomic ratio on the afterglow properties of red-emitting CaS:Eu^{2+},Pr^{3+} phosphors *J. Ceramic Processing Research* **14** s57-s59

[24] Kojima Y, Takahashi A and Umegaki T 2014 Synthesis of orange-red-emitting Eu^{2+},Pr^{3+} codoped SrS long afterglow phosphor *J. Lumin.* **146** 42-45

[25] Rodriguez Burbano D C, Sharma S K, Dorenbos P, Viana B and Capobianco J A 2015 Persistent and photostimulated red emission in CaS:Eu^{2+},Dy^{3+} nanophosphors *Adv. Optical Mater.* **3** 551-557

[26] Inoue Y, Okamoto M and Morimoto J 2006 Superimposed emissions on enhanced green emission from ZnO:Pr powders by evacuated sealed silica tube method *Jpn. J. Appl. Phys.* **45** 4128-4130

[27] Nanai Y, Suzuki K and Okuno T 2015 Crystal structure and photoluminescence of $(Gd,Ce)_4(SiS_4)_3$ and $(Y,Ce)_4(SiS_4)_3$ *Materials Research Express* **2** 036203(11pp)

[28] Nanai Y, Suzuki Y and Okuno T 2016 Efficient host excitation in thiosilicate phosphors of lanthanide(III)-doped $Y_4(SiS_4)_3$ *Journal of Physics D: Applied Physics* **49** 105103(8pp)

[29] Nanai Y, Kamioka H and Okuno T 2018 Broad luminescence of Ce^{3+} in multiple sites in $(La,Ce,Y)_6Si_4S_{17}$ *Journal of Physics D: Applied Physics* **51** 135103(8pp)

[30] Dieke G H 1968 *Spectra and energy levels of rare earth ions in crystals* (New York: John Wiley & Sons)

[31] Randall J T, Wilkins M H F 1945 Phosphorescence and electron traps I The study of trap distributions, *Proc. Roy. Soc. A* **184** 365-389

[32] Randall J T, Wilkins M H F 1945 Phosphorescence and electron traps II The interpretation of long period phosphorescence, *Proc. Roy. Soc. A* **184** 390-407

[33] McKeever S W S 1985 *Thermoluminescence of solids* (Cambridge University Press)

[34] Hoogenstraaten 1958 Electron traps in ZnS phosphors, *Philips Research Reports* **13** 515-693

[35] Avouris P and Morgan T N 1981 A tunneling model for the decay of luminescence in inorganic phosphors: The case of Zn_2SiO_4:Mn, *J. Chem. Phys.* **74** 4347-4355

[36] Suda Y, Kamigaki Y and Yamamoto H 2018 Blue emission in photoluminescence spectra of the red phosphor $CaAlSiN_3:Eu^{2+}$ at low Eu^{2+} concentration, *J. Appl. Pys.* **123** 161542(9pp)

[37] Suda Y, Kamigaki Y, Miyagawa H, Takeda T, Takahashi K, Hirosaki N 2020 Luminescence and afterglow due to defects in β-SiAlON crystal powder, submitted

[38] Ren Y, Yang Z, Li M, Ruan J, Zhao J, Qiu J, Song Z and Zhou D 2019 Reversible upconversion luminescence modification based on photochromism in $BaMgSiO_4:Yb^{3+},Tb^{3+}$ ceramics for anti-counterfeiting application, *Adv. Optical Matter.* **7** 1900213(12pp)

[39] Yamashita N, Fukumoto S, Ibuki S and Ohnishi H 1993 Photoluminescence of Eu^{2+} and Eu^{3+} centers in CaS:Eu,Na phosphors, *Jpn. J. Appl. Phys.* **32** 3135-3139

[40] Takahashi K, Kohda K, Miyahara J, Kanemitsu Y, Amitani K, Shionoya S 1984 Mechanism of photostimulated luminescence in $BaFX:Eu^{2+}$ (X=Cl,Br) phosphors *J. Lumin.* **31-32** 266-268

[41] Hao Z, Zhang J, Zhang X, Wang X 2011 $CaSc_2O_4:Eu^{3+}$: A tunable full-color emitting phosphor for white light emitting diodes *Opt. Mater.* **33** 355-358

[42] Brightwell J W, Ray B and Buckley C N 1982 Preparation, crystal growth and luminescence in calcium sulphide *J. Crystal Growth* **59** 210-216

Figure captions

Figure 1 XRD patterns of $CaS:Eu^{2+},Tm^{3+}$. The concentration of Eu^{2+} is shown in the figure. At the lower part of the figure, the reference data of CaS, Tm_2O_3 and CaO are included.

Figure 2 PL (right) and PLE (left) spectra of $CaS:Eu^{2+},Tm^{3+}$. The concentration of Eu^{2+} is shown in the figure. The PL peak wavelength is used for obtaining PLE spectra.

Figure 3 Internal quantum efficiency plotted against the concentration of Eu^{2+} in $CaS:Eu^{2+},Tm^{3+}$.

Figure 4 Temporal decays of persistent luminescence of $CaS:Eu^{2+},Tm^{3+}$. The concentration of Eu^{2+} is shown in the figure.

Figure 5 TL glow curves of $CaS:Eu^{2+},Tm^{3+}$. The concentration of Eu^{2+} is shown in the figure. Heating rate is 5 K/min.

Figure 6 Excitation spectrum of persistent luminescence of $CaS:Eu^{2+},Tm^{3+}$. The concentration of Eu is 0.05%. The excitation is carried out using monochromatic output of a xenon arc lamp. The intensity of persistent luminescence 150 s after ceasing of the photoexcitation, which is normalized by the intensity of the photoexcitation, is potted against the wavelength of the photoexcitation.

Figure 7 TL glow curves of $CaS:Eu^{2+},Tm^{3+}$ measured under three heating rates shown in the figure. The concentration of Eu is 0.05%. The excitation is carried out using (a) a mercury lamp (254 nm) or (b) a blue LED (470 nm).

Figure 8 Hoogenstraaten plots obtained from TL glow curves of CaS:Eu^{2+},Tm^{3+}. The concentration of Eu^{2+} is 0.05%. The calculated trap depth is 0.27 eV for the excitation using the mercury lamp (254 nm) or 0.33 eV using the blue LED (470 nm).

Figure 9 Temporal PL spectra of CaS:Eu^{2+},Tm^{3+} measured at 15K. The concentration of Eu^{2+} is 0.05% or 1%. Excitation is made using 10 ns pulses, and its wavelength is 266 nm. Sampling of PL started at 20 ns after the pulse excitation, and the duration was 50 μs.

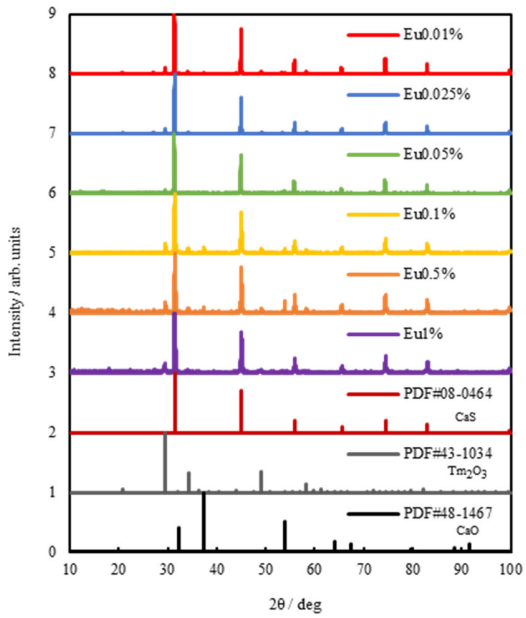

Figure 1

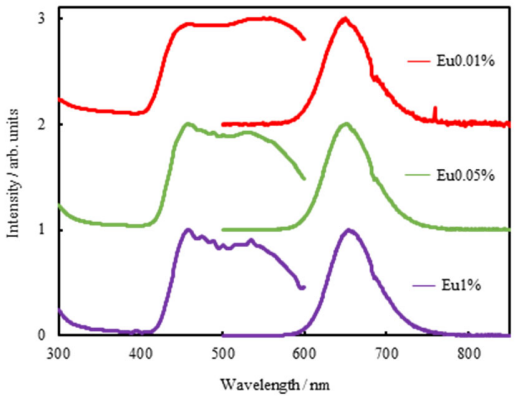

Figure 2

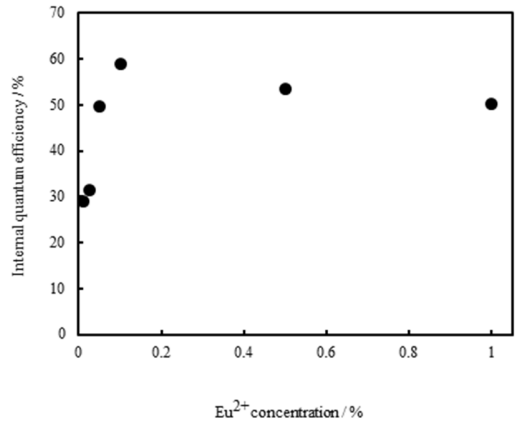

Figure 3

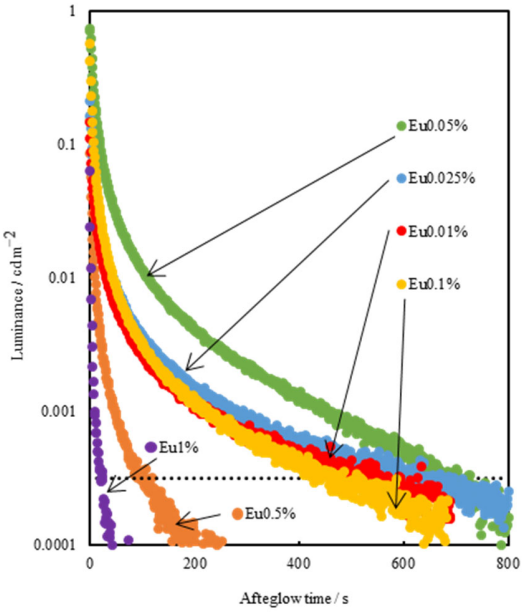

Figure 4

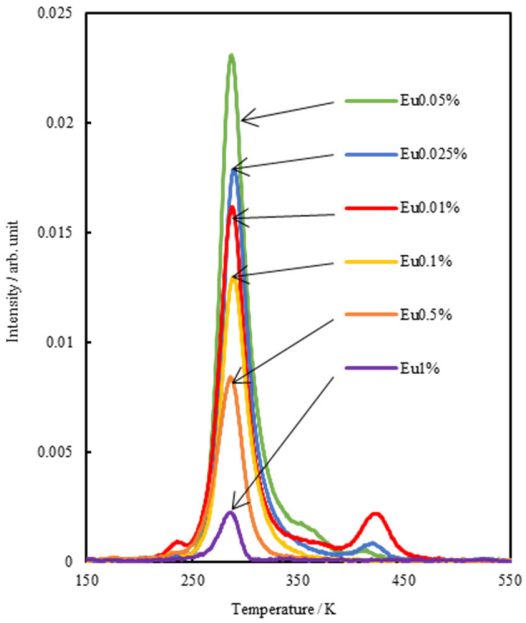

Figure 5

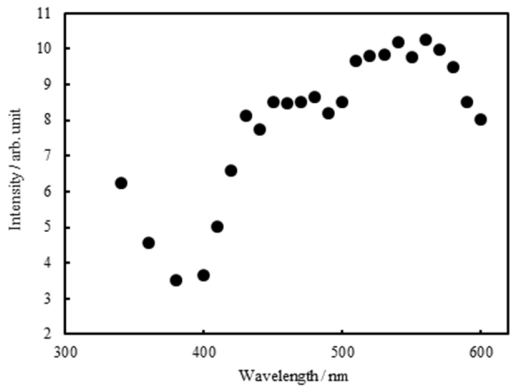

Figure 6

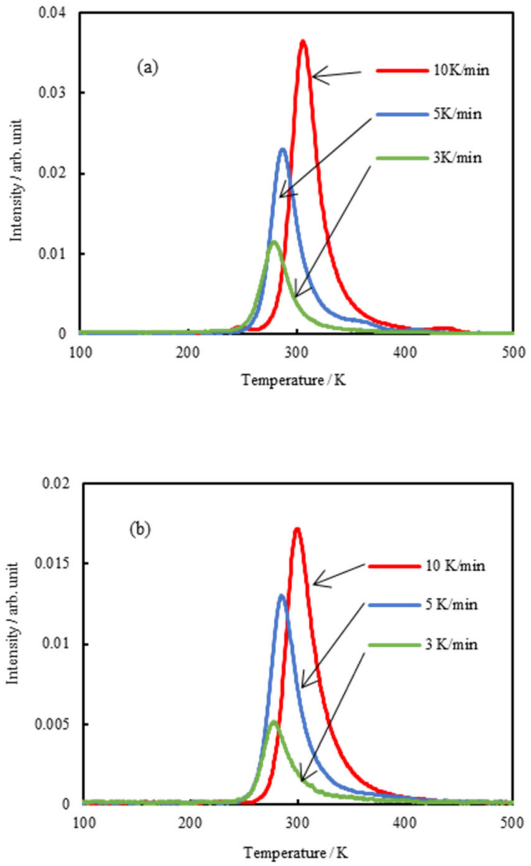

Figure 7

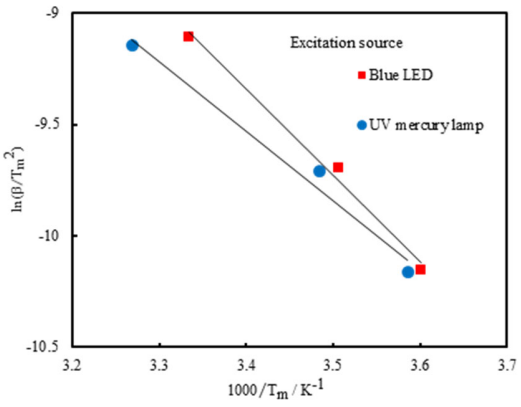

Figure 8

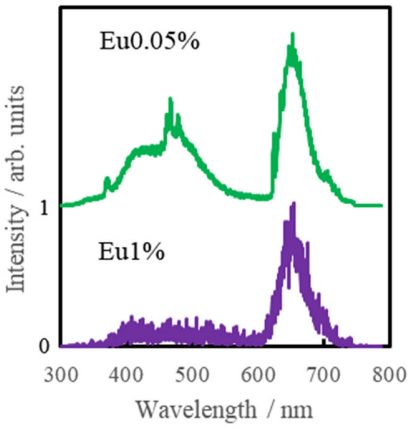
Eu0.05%
Eu1%
Intensity / arb. units
1
0
300
400
500
600
700
800
Wavelength / nm

Figure 9